Wavelet level decomposition of the seismic response of a historic masonry bell tower with and without simulated structural damage

Available online at www.sciencedirect.com

ScienceDirect

Procedia Structural Integrity 44 (2023) 1562–1569

Structural Integrity Procedia

www.elsevier.com/locate/procedia

XIX ANIDIS Conference, Seismic Engineering in Italy

Wavelet level decomposition of the seismic response of a historic masonry bell tower with and without simulated structural damage

Marco Civera[a]*, and Cecilia Surace[a]

[a]*Politecnico di Torino, Department of Structural, Building and Geotechnical Engineering, Corso Duca degli Abruzzi, 24, 10129, Turin, Italy*

Abstract

Historical buildings are of foremost importance due to their unique and irreplaceable value. However, their ageing structure and materials make them particularly vulnerable to structural damage. This may result in catastrophic failure under strong motions, which are unfortunately not uncommon in seismic areas such as Italy. This numerical study discusses the application of Wavelet Level Decomposition (WLD) to the seismic response of such historical structures. The simulated data are obtained from a calibrated Finite Element (FE) model of the Santa Maria and San Giovenale Cathedral bell tower in Fossano (Northern Italy). This structure suffered major structural damage during an earthquake in 1887; it then underwent several interventions, the last one being in 2012. It is also currently scheduled for further reinforcement works in the near future. The FE analyses consider a set of realistic earthquake inputs in accordance with the seismic hazard zone of Fossano, with and without damage (modelled as a stiffness reduction in the façades, considering several possible crack patterns). The results show the potential for WLD-based retrospective analysis after seismic events on recorded signals.

Keywords: wavelet analysis; discrete wavelet transform; multiresolution analysis; earthquake engineering; cultural heritage.

* Corresponding author.
E-mail address: marco.civera@polito.it

10.1016/j.prostr.2023.01.200

1. Introduction

The architectural and historical heritage is constantly at risk of structural failure due to ageing building materials and slowly decreasing mechanical properties. Nevertheless, the Structural Health Monitoring (SHM) of such structures requires particular attention for the preservation of their aesthetics and original characteristics (De Stefano et al., 2016). Vibration-based Inspection (VBI) can be seen as a minimally-invasive yet effective option. Nevertheless, the unrefined use of acceleration time histories might not be sensitive enough to detect damage at an early development stage.

In this context, Mallat's pyramidal algorithm for Discrete Wavelet Transform (DWT, (Mallat, 1989)) can be applied to decompose the original signal into several multiresolution components, known as *wavelet levels* (WLs). In fact, each level corresponds to a different resolution, as the signal is filtered and downsampled at each step. This has been proved capable to provide a reliable tool for signal decomposition in the field of damage detection, with previous applications to rolling element bearings documented in the scientific literature (Ziaja et al., 2014). However, this approach does not seem to have been tested for masonry structures in general or for large historical structures in particular.

The concept is that a subset of these levels can be then properly selected according to their sensitivity to damage, retaining the most useful ones. The other levels, which are less affected by damage and/or more impacted by other confounding influences such as measurement noise, can be removed. This allows for a sort of denoising, enhancing damage detection directly in the time domain.

Here, the proposed methodology is validated over the case study of the Santa Maria and San Giovenale Cathedral bell tower in Fossano (Italy). Several damage scenarios, designed accordingly to common crack patterns encountered in post-earthquake surveys of similar buildings, are considered. These are applied to a calibrated Finite Element (FE) model. The response of the model is then evaluated considering realistic strong motions. The results of these numerical tests highlight the potentialities of the variance of selected WLs as a damage index.

2. Discrete Wavelet Transform and Wavelet Levels

Although the background theory about wavelets is well known, a brief recall is included here for completeness. Independently from the specific kind of mother wavelet $\psi(t)$ considered, the Wavelet Transform (WT) of a signal $x(t)$ is a linear transform into a scale j and a translation k domain. This transform can be defined as

$$x_{j,k} = \int_{-\infty}^{+\infty} x(t)\psi_{j,k}(t)\,dt \tag{1}$$

where $\psi_{j,k}$ can be any (in this case, time-dependent) function that satisfies a few specific requirements (detailed in (Daubechies, 1992)). Differently from the Fourier Transform, $\psi(t)$ is time localised; this allows the representation of nonstationary signals as well. This property becomes useful for the analysis of seismic responses, where the external excitation has a relatively short duration and rapid, heteroskedastic variations.

To avoid redundancy, orthogonal wavelets are needed. For this research, the well-known Daubechies wavelets (Daubechies, 1988) have been considered, due to their extensive use for similar purposes in signal processing (see e.g. (Staszewski et al., 1999; Ziaja et al., 2014)). Their main property is to have the largest possible number of vanishing moments p for a support of length $(2p - 1)$. The value of p can be set arbitrarily, considering that the lowest case ($p = 1$) yields a square-wave expansion basis, known as the Haar wavelet, while higher orders return a more complexly-shaped waveform. Specifically, after some testing, the order 'd4' was selected. This corresponds to $p = 4$ vanishing moments, for a total filter length of 8 (this is important as other authors, see e.g. (Ziaja et al., 2014), follow the convention to use the filter length to indicate the order). Overall, this satisfies the general 'rule of thumb' of applying low-order Daubechies wavelets for fast-changing signals.

In the case of Discrete Wavelet Transform (DWT), a set of scale and translation parameters is applied, obtained from a dyadic grid defined by $a = 2^j$ and $b = k2^j$, such that the child wavelets become

$$\psi_{j,k}(t) = \frac{1}{\sqrt[2]{a}}\psi\left(\frac{t-b}{a}\right) \tag{2}$$

where the term $\frac{1}{\sqrt[2]{a}}$ ensures the energy independence for each wavelet level. This discretised version of WT is important as it allows to halve the signal at each level, in the cascading fashion of Mallat's algorithm.

The rationale for WT in general and DWT in particular is that the original signal can be represented as the linear sum of properly scaled and translated $\psi_{j,k}(t)$. That is to say, for a (theoretically) infinite signal, one would have

$$x(t) = \sum_j^\infty \sum_k^\infty D_{j,k}\psi_{j,k}(t) + A_0 \tag{3}$$

where $D_{j,k}$ indicates the so-called detail coefficients and A_0 is the mean of the signal. Each $D_{j,k}$ coefficient multiplies its corresponding child wavelet, scaled according to j and translated according to k. This corresponds to a full decomposition of $x(t)$. In the end, if the recorded time series is made exactly by 2^N timesteps, this results in $N+1$ levels of increasing resolution. The first two levels, '-1' and '0', are obtained at the end of the cascade process and represent the last remaining approximation and detail coefficient, in the same order (i.e. the aforementioned A_0 and D_0). In other words, level -1 is the remaining constant value needed to address non-zero-mean signals (as all wavelets are strictly required to have a null mean (Daubechies, 1992)). All the higher levels, instead, will be defined over 2^j basis functions, up to $N-1$ – e.g. Level 0 is made up of a single (2^0) modulated wavelet.

Nevertheless, one can stop the signal reconstruction process at any step, obtaining instead

$$x(t) = \sum_j^M \sum_k^\infty D_{j,k}\psi_{j,k}(t) + \sum_j^M \sum_k^\infty A_{j,k}\varphi_{j,k}(t) \tag{4}$$

where $\varphi_{j,k}(t)$ indicates the quadrature mirror filter of $\psi_{j,k}(t)$ and the terms $A_{j,k}$ are known as the approximation coefficients. This corresponds to a removal of the highest levels, which are the ones focused on the shortest wavelet scales and therefore the highest frequencies. For this reason, this process is widely used as a denoising technique. Nevertheless, one is not strictly required to reconstruct the signal from the lowest level, bottom-up; any intermediate decomposition step can be used to reconstruct a signal component. That is to say, it is possible to define, for any j,

$$x_j(t) = \sum_k^\infty D_{j,k}\psi_{j,k}(t) \tag{5}$$

as the component of the signal made up of all the child wavelets with the same scale $a = 2^j$, translated along t and modulated by their respective detail coefficients. This is the definition of *wavelet level* as intended here.

As one can easily understand, lower levels will be focused on low-frequency trends, while higher WLs will capture more rapid, high-frequency variations (generally also including noise in their highest levels).

Hence, the energy content of interest – i.e. the structure's vibrational response, detrended and denoised – is expected to be mostly confined on some midway levels. These can be then isolated and seen as a structure-specific dynamic signature; any damage-induced alterations of the system's dynamics will be largely reflected on them while having a negligible impact on higher and lower WLs.

To evaluate these damage effects, the WL variance, σ_j^2, represents an easy-to-use and efficient metric. By way of example, the first decomposition step (corresponding to WL $(N-1)$) of the finite signal introduced above will a finite set of $N/2$ timesteps. Its variance can be defined as

$$\sigma_{j=N-1}^2 = \frac{1}{N/2}\sum_{i=1}^{N/2}\left(x_{j=N-1}[i] - \mu\right)^2 \tag{6}$$

while the total energy of the same is

$$\sum_{i=1}^{N/2}\left(x_{j=N-1}[i]\right)^2 \tag{7}$$

thus, Eq. (7) is directly proportional to Eq. (6) if a zero-mean signal is assumed; as said, all WLs have a null mean ($\mu = 0$) by definition.

Importantly, σ_j^2 is (at least theoretically) insensitive to ambient vibrations and other damage-unrelated

phenomena. In fact, due to the scale invariance of random processes, a stationary white Gaussian noise (WGN) would have flat energy distribution for all WLs; henceforth, (almost) identical variance $\sigma_j^2 \ \forall j$. This links closely the theory of wavelet multiresolution analysis and entropy, as already suggested in (Ziaja et al., 2014); in fact, the disruption of entropy has been proposed as well in several cases as a mean for anomaly (and thus, damage) detection (Ceravolo et al., 2019, 2021; Civera & Surace, 2022).

However, the recorded structural response is not a WGN. Thus, its WL variance is supposed to be unequally distributed among the different levels, reflecting the distribution of the output energy spectrum in the frequency domain. This unequal distribution, however, is supposed to remain unaltered for the same structure if excited by comparable inputs. Thus, if similar driving forces are applied, any anomaly in the distribution of σ_j^2 for the several $j = 0,1,2, \dots, N-1$ (neglecting $j = -1$) can be linked to a structural anomaly in the investigated system. This is, essentially, a classic application of the Statistical Pattern Recognition approach to SHM proposed by (Farrar et al., 2001). In conclusion, the aim is to compare the σ_j^2 distribution of the recorded response to a known baseline, looking for statistically-relevant deviations.

3. Case Study

The bell tower of the Santa Maria and San Giovenale Cathedral in Fossano (Fig. 2.a) was the subject of several recent studies (Civera et al., 2019, 2021; Ferraris et al., 2020), where a detailed description can be found. From an engineering perspective, the masonry tower (built 1389-1420) is 35 m high, with a wall thickness ranging from a minimum of 0.5 m (belfry) to a maximum of 1.5 m (base). The 11 orders of steel ties visible in Fig. 2.a are in place since the last reinforcement interventions in 2012.

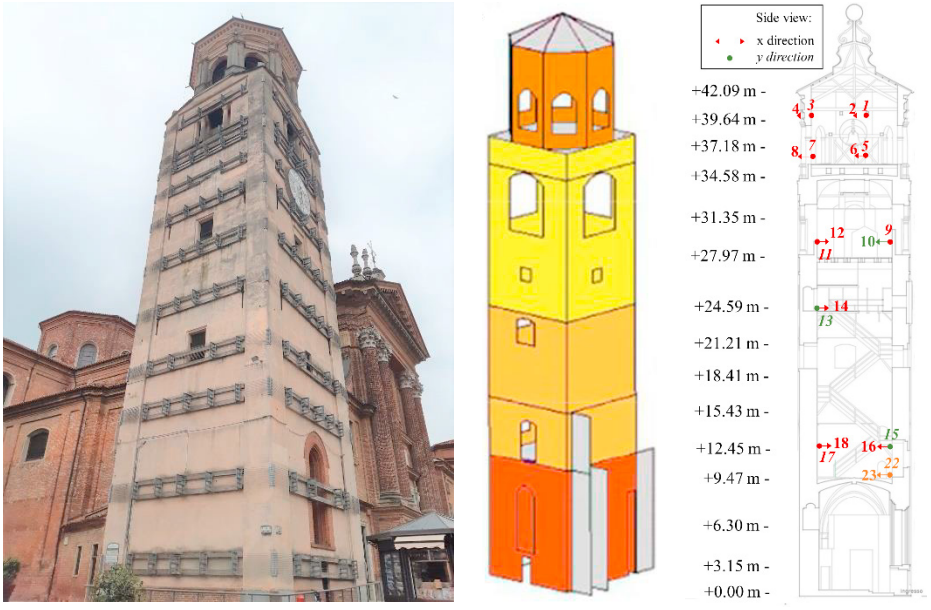

(a) (b) (c)

Fig. 1. (a) picture of the Santa Maria and San Giovenale Cathedral bell tower as seen from a recent survey (May 2022). (b) finite element model (in ANSYS Mechanical APDL, version 17.2) with the macro-areas highlighted. (c) structural scheme with the sensor layout considered here.

3.1. Finite Element Model and Analysis

The FE model portrayed in Fig. 1.b has been utilised for this work; the model was calibrated accordingly to the results of the last survey available (Ceravolo et al., 2016) to be representative of the current structure 'as is'. To accommodate for the difference between the residual properties of the partially damaged materials at different heights, the four macro-elements were set with different values of Young's modulus. Specifically, from the ground

up, these are: $E_0 = 2.69\ 10^3$ MPa (storey level 0), $E_1 = 1.32\ 10^3$ MPa (level 1), $E_2 = 1.25\ 10^3$ MPa (level 2), and $E_3 = 2.47\ 10^3$ MPa (level 3). This reflects the relatively larger damage encountered on the external façades at mid-height. The other parameters (Poisson's ratio $\nu = 0.30$, density $\rho = 2000$ kg/m^3, and viscous damping $\xi = 5\%$) were assumed as constant throughout the whole structure. 8-noded, 6 DoF-per-node rectangular shell elements were used everywhere. The connections at the tower base with the nearby cathedral were modelled as linear spring elements (coloured in light grey in Fig. 1.b).

The sensor layout reproduced in Fig. 1.c was simulated considering the nodes closest to the corresponding accelerometers and only taking the direction of the actual output channels. In the experimental survey, three layouts of 18 sensors were considered, maintaining 15 accelerometers as reference (red arrows) while changing the remaining three (green arrows). This layout corresponds to a hybrid of the 1st setup plus two channels (#22 and #23, in orange) from the 3rd setup.

For the input, spectrum-compatible earthquakes were artificially generated employing the SIMQKE software (Gasparini & Vanmarcke, 1990) following the Italian normative requirements. The seismic intensity parameters reported in Table 1 (more details available in (Ferraris et al., 2020)) were considered, also according to the Cathedral location (Long=7.725, Lat=44.549). For simplicity, only the two horizontal components (applied in the x- and y-directions) were applied, neglecting the vertical component. According to the Limit State Design approach of the Italian normative, the limit state for the safeguard of life (*Stato Limite di salvaguardia della Vita*/SLV) was considered. The total duration was set to 35 s; to provide some variability in the dataset, the stationary part of the simulated spectrum-compatible earthquakes was varied between 10 s and 25 s, in accordance with NTC 2018 §3.2.3.6 (*Norme Tecniche per Le Costruzioni 2018 (NTC 2018)*, 2018). 10 earthquakes per case (enlisted in the next subsection) were generated. The system response was firstly simulated with $f_s = 100$ Hz, then resampled to have exactly 1024 timesteps (corresponding to $N = 10$ levels, discarding Level -1 as mentioned earlier).

Table 1. Seismic intensity parameters, according to the Italian regulation (NTC 2018).

Parameter	Value
Return period	$T_r = 475$ years
Peak (horizontal) ground acceleration	$a_g = 0.109\ g$
Soil category	C ($S_s = 1.50$, $C_c = 1.59$)
Topographic category	$T1$ ($S_t = 1.00$)

3.2. Simulated damage patterns

To test the SHM procedure, the response of the baseline structure ('as is') needed to be compared with some damage scenarios. The ones considered here (enlisted in Table 2 and portrayed in Fig. 2) are representative of realistic crack patterns commonly encountered on masonry towers and bell towers after major seismic events – see e.g. (Coïsson et al., 2017).

Table 2. Baseline model and other scenarios for numerical validation.

Case number	Name	Description
01 to 04	healthy sets (#1 to #4)	Baseline FE model as calibrated ('as is'), with different seismic inputs
05	altered #1: +1.00%	Global increase of all the masonry levels (E_0, E_1, E_2, E_3) of +1%
06	altered #2: + 0.25%	Global increase of all the masonry levels (E_0, E_1, E_2, E_3) of +0.25%
07	altered #3: -1.00%	Global increase of all the masonry levels (E_0, E_1, E_2, E_3) of -1%
08	altered #4: -0.25%	Global increase of all the masonry levels (E_0, E_1, E_2, E_3) of -0.25%
09	realistic damage #1	15.00% reduction of E_0 (all four façades as highlighted in Fig. 2.a)
10	realistic damage #2	15.00% reduction of E_0 and E_1 in the sections highlighted in Fig. 2.b
11	realistic damage #3	15.00% reduction of E_0, E_1, and E_3 in the sections highlighted in Fig. 2.c
12	realistic damage #4	15.00% reduction of E_2 and E_3 in the sections highlighted in Fig. 2.d

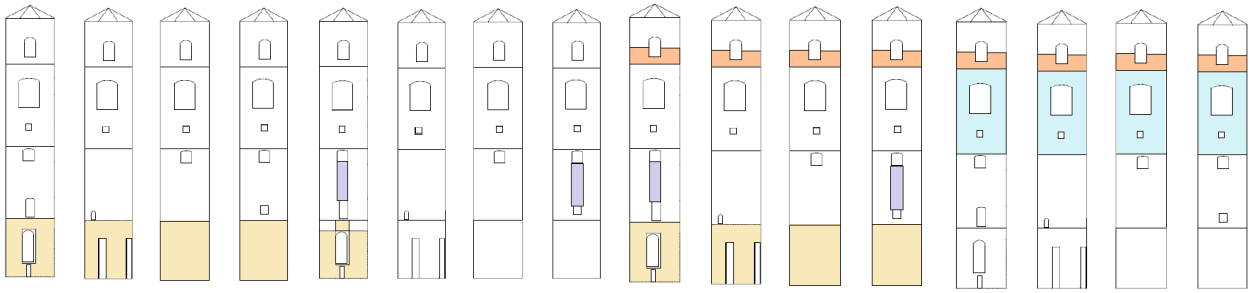

Fig. 2. The four realistic damage scenarios, as defined accordingly to crack patterns encountered on similar structures damaged by earthquakes. The coloured areas indicate the portion with reduced Young's modulus.

4. Results

To highlight the share of total energy distributed for each WL, the WL variances σ_j^2 are normalised over the whole signal variance σ^2. Since $\sigma^2 = \sum \sigma_j^2$, $\widehat{\sigma_j^2} = \sigma_j^2/\sigma^2 \in [0,1] \; \forall j$.

Only by way of example, the results from channel #22 (close to the bell tower base) are portrayed in Fig. 3. The same overall trends were encountered in all cases, regardless of the specific sensor location and orientation. Level -1 is reported for completeness, even if the variance of a constant value is, of course, null by definition. In the case of the structure 'as is' or slightly altered, the predominant part of the response energy is localised in $j = 6$ and, to a much lesser extent, in the neighbouring WLs. Vice versa, this energy content is mostly transferred to $j = 5$ for increasing damage. All the other levels account for a negligible amount of variance. This downward trend was expected due to the reduced stiffness. As the natural frequencies of the structure decrease, most of the power spectrum shifts to the lower frequencies. In the decomposed time-domain signal, this causes a detectable variation in the Wavelet Level Variance, which can be seen and used as a damage-sensitive feature. In the particular case represented in Fig. 3, the response energy allocation of the four datasets corresponding to the baseline was $78 \pm 7\%$ in WL6 and $18 \pm 5\%$ in WL5 (the remaining ~4% being mostly included in WL7). For the four datasets with slight variations, intended to mimic statistical fluctuations in the material properties and not actual damage, this ratio shifted to $78 \pm 5\%$ and $20 \pm 4\%$ (WL6 and WL5, in the same order). As expected, the variance of WL7 slightly increased for the two cases with $+0.75\%$ and $+1.00\%$ Young's modulus applied to the structure. Nevertheless, these changes are quite minimal and thus cannot be considered indicative of damage beyond any reasonable doubt. Conversely, the four scenarios with realistic damage patterns induced more marked variations, as $65 \pm 13\%/32 \pm 13\%$ (WL6/WL5). In general, this corresponds to a $\Delta\sigma_{j=5} = +205.6\%$ increase for WL5 and a $\Delta\sigma_{j=6} = -16.7\%$ decrease for WL6.

More in detail, the third realistic case, with its damage all around the bell tower base, the belfry, and partially on the first floor, returned the strongest deviation from the baseline. The effects of the second case, with a similar damage pattern (yet limited to the main façade and with no cracks at the belfry), seem to be closer to the normality condition, even if still differentiated enough. The same can be said for the first case as well (with damage only at the base, for all four façades). Even the last (fourth) damage scenario, with extensive damage but located solely on the upper half of the tower, returned a relatively less pronounced yet still clearly visible effect, also on the sensors closer to the ground level.

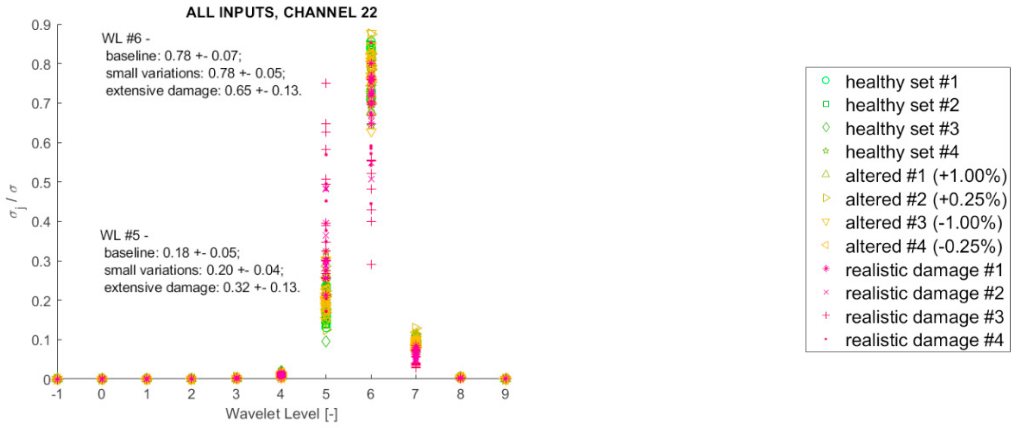

Fig. 3. Results for output channel #22.

5. Conclusions

This short paper presented an application of wavelet-based self-similarity analysis to historical masonry structures, aiming at damage detection under earthquake excitation. The rationale for the proposed approach is that the occurrence of damage alters the energy distribution of a target system among its wavelet levels, where each one of these levels corresponds to a specific wavelet scale. This was tested for the numerically simulated response of the Santa Maria and San Giovenale Cathedral bell tower in Fossano, considering realistic strong motions. This case study was endangered by seismic activity throughout the last centuries and is of renewed interest, as it is due to reinforcement works in the near future.

Overall, the results showed that the content of actual interest is strongly localised in the recorded time series, with only two wavelet levels comprising most of the damage-induced variation. Furthermore, these alterations were clearly visible in the target WLs, highlighting that

(i) the variance of carefully chosen WL can be reliably used for damage assessment, and
(ii) the simulated damage patterns cause a potentially dangerous anomaly in the bell tower dynamics in case of an incoming earthquake.

Considering this last aspect, the numerical simulations performed in this study will be important as well to validate the expected improvement of potential new reinforcement interventions, like the ones planned for the particular case study considered here. In this regard, the type, location, and size of such reinforcements can be optimised for the current structure to match the expected response of its original (pristine) counterpart to strong motions. This potential use will be better investigated in future works.

Acknowledgements

the Authors wish to thank Prof Rosario Ceravolo, Dr Gaetano Miraglia, and Dr Erica Lenticchia for providing the Finite Element Model of the Fossano Bell Tower.

References

Ceravolo, R., Civera, M., Lenticchia, E., Miraglia, G., & Surace, C. (2021). Detection and classification of multiple damages through entropy. *Applied Sciences*.

Ceravolo, R., Lenticchia, E., & Miraglia, G. (2019). Spectral entropy of acceleration data for damage detection in masonry buildings affected by seismic sequences. *Construction and Building Materials*, *210*, 525–539. https://doi.org/10.1016/j.conbuildmat.2019.03.172

Ceravolo, R., Pistone, G., Fragonara, L. Z., Massetto, S., & Abbiati, G. (2016). Vibration-Based Monitoring and Diagnosis of Cultural Heritage: A Methodological Discussion in Three Examples. *International Journal of Architectural Heritage*, *10*(4), 375–395.

https://doi.org/10.1080/15583058.2013.850554

Civera, M., Ferraris, M., Ceravolo, R., Surace, C., & Betti, R. (2019). The Teager-Kaiser Energy Cepstral Coefficients as an Effective Structural Health Monitoring Tool. *Applied Sciences*, *9*(23), 5064. https://doi.org/10.3390/app9235064

Civera, M., Pecorelli, M. L., Ceravolo, R., Surace, C., & Zanotti Fragonara, L. (2021). A multi-objective genetic algorithm strategy for robust optimal sensor placement. *Computer-Aided Civil and Infrastructure Engineering*, mice.12646. https://doi.org/10.1111/mice.12646

Civera, M., & Surace, C. (2022). Instantaneous Spectral Entropy: An application for the Online Monitoring of Multi-Storey Frame Structures. *Buildings*, *12*(3). https://doi.org/10.3390/buildings12030310

Coïsson, E., Ferretti, D., & Lenticchia, E. (2017). Analysis of damage mechanisms suffered by Italian fortified buildings hit by earthquakes in the last 40 years. *Bulletin of Earthquake Engineering*, *15*(12), 5139–5166. https://doi.org/10.1007/S10518-017-0172-0/FIGURES/10

Daubechies, I. (1988). *Orthonormal Bases of Compactly Supported Wavelets*.

Daubechies, I. (1992). *Ten lectures on wavelets*. Society for Industrial and Applied Mathematics.

De Stefano, A., Matta, E., & Clemente, P. (2016). Structural health monitoring of historical heritage in Italy: some relevant experiences. *Journal of Civil Structural Health Monitoring*, *6*(1), 83–106. https://doi.org/10.1007/s13349-016-0154-y

Farrar, C. R., Doebling, S. W., & Nix, D. A. (2001). Vibration–based structural damage identification. *Philosophical Transactions of the Royal Society of London. Series A: Mathematical, Physical and Engineering Sciences*, *359*(1778), 131–149. https://doi.org/10.1098/rsta.2000.0717

Ferraris, M., Civera, M., Ceravolo, R., Surace, C., & Betti, R. (2020). *Using Enhanced Cepstral Analysis for Structural Health Monitoring* (pp. 150–165). Springer, Singapore. https://doi.org/10.1007/978-981-13-8331-1_11

Gasparini, D., & Vanmarcke, E. H. (1990). *SIMQKE: A program for artificial motion generation*.

Mallat, S. G. (1989). A Theory for Multiresolution Signal Decomposition: The Wavelet Representation. In *IEEE TRANSACTIONS ON PATTERN ANALYSIS AND MACHINE INTELLIGENCE: Vol. II* (Issue 7). https://doi.org/10.1109/34.192463

Norme Tecniche per le Costruzioni 2018 (NTC 2018). (2018).

Staszewski, W., Ruotolo, R., & Storer, D. (1999). Fault Detection in Ball-bearings Using Wavelet Variance. *Proceedings of the 17th International Modal Analysis Conference (IMAC)*, 1335.

Ziaja, A., Antoniadou, I., Barszcz, T., Staszewski, W. J., & Worden, K. (2014). Fault detection in rolling element bearings using wavelet-based variance analysis and novelty detection: *Journal of Vibration and Control*, *22*(2), 396–411. https://doi.org/10.1177/1077546314532859